Probing the photon emissivity of thermal QCD matter on the lattice

Harvey Meyer
Johannes Gutenberg University Mainz

Lattice@CERN2024 workshop, CERN, 8 July 2024

This talk is mainly based on the following publications:

1. 2001.03368 (PRD): *Rate of photon production in the quark-gluon plasma from lattice QCD*,
   Marco Cè, Tim Harris, HM, Aman Steinberg, Arianna Toniato.

2. 2205.02821 (PRD): *Photon emissivity of the quark-gluon plasma: A lattice QCD analysis of the transverse channel*,
   Marco Cè, Tim Harris, Ardit Krasniqi, HM, Csaba Török.

3. 2309.09884 (PRD): *Probing the photon emissivity of the quark-gluon plasma without an inverse problem in lattice QCD*,
   Marco Cè, Tim Harris, Ardit Krasniqi, HM, Csaba Török.

Brief advertisement for our recent preprint:

4. 2407.01657: *Hot QCD matter around the chiral crossover: A lattice study with O(a)-improved Wilson fermions*,
   Ardit Krasniqi, Marco Cè, Renwick Hudspith, HM.

Motivation (I): heavy-ion collision phenomenology

- direct photons (those not produced via hadronic decays) encode information about the environment in which they were created
- for $1\mathrm{GeV} \lesssim p_T \lesssim 2\mathrm{GeV}$: expect a dominant contribution from (quasi-)thermal photons: quark-gluon plasma and hadronic phase

ALICE [2308.16704]

- Used measurement of e^+e^- pairs with $m_{ee} < 30\,$MeV: fraction of direct/inclusive dielectrons is the same as for photons.

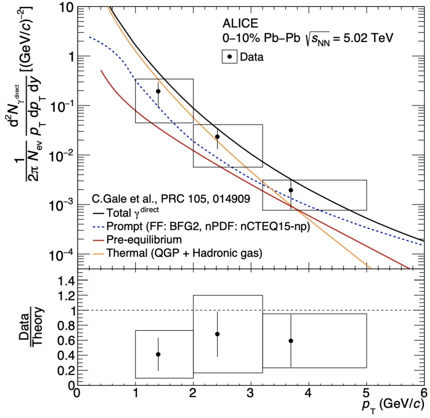

Photon emissivity and thermal vector spectral functions

$$\rho^{\mu\nu}(\mathcal{K}) = \int d^4x\, e^{i\mathcal{K}\cdot x}\, \frac{1}{Z}\sum_n e^{-E_n/T}\langle n|[j^\mu(x), j^\nu(0)]|n\rangle$$

- Rate of dilepton production per unit volume plasma: [McLerran, Toimela 1985]

$$d\Gamma_{\ell^+\ell^-}(\mathcal{K}) = \alpha^2\, \frac{d^4\mathcal{K}}{6\pi^3\mathcal{K}^2}\, \frac{-\rho^\mu{}_\mu(\mathcal{K})}{e^{\beta\mathcal{K}^0}-1} \qquad (\mathcal{K}^2 \equiv \omega^2 - k^2)$$

- Rate of photon production per unit volume plasma:

$$d\Gamma_\gamma(\boldsymbol{k}) = \alpha\, \frac{d^3k}{4\pi^2\, k}\, \frac{-\rho^\mu{}_\mu(k,\boldsymbol{k})}{e^{\beta k}-1}.$$

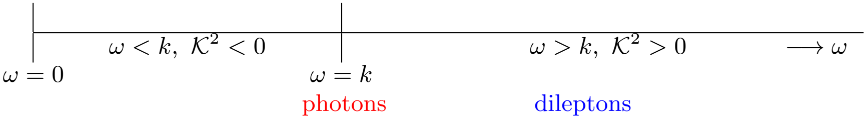

Predictions for $\sigma(\omega = k) = -\frac{1}{2}\rho^{\mu}{}_{\mu}(k, \boldsymbol{k})$ in non-Abelian plasmas:

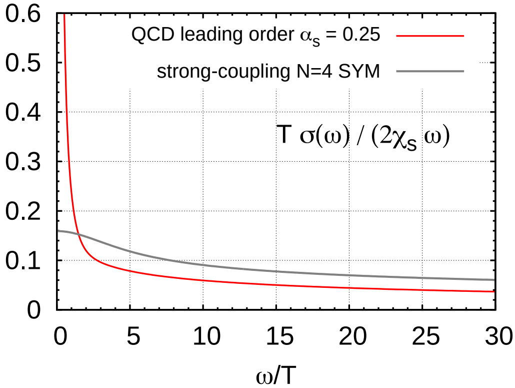

Motivation (II)

intercept $= T \cdot D$,

$D =$ diffusion coefficient.

- $\sigma(\omega)$ vanishes in the vacuum;
- at $\omega \neq 0$ it vanishes for thermal, non-interacting quarks;
- ideal probe of the medium!

Arnold, Moore Yaffe JHEP 11 (2001) 057 and JHEP 12 (2001) 009.
AdS/CFT: Caron-Huot et al. JHEP 12 (2006) 015.

A one-parameter family of expressions for the photon emissivity

- at finite temperature, there are two independent, O(3) invariant components: $(k \equiv |\boldsymbol{k}|, \quad \hat{k}^i = k^i/k)$

$$\rho_L(\omega, k) \equiv (\hat{k}^i \hat{k}^j \rho^{ij} - \rho^{00}), \qquad \rho_T(\omega, k) \equiv \frac{1}{2}(\delta^{ij} - \hat{k}^i \hat{k}^j)\rho^{ij}.$$

- current conservation: $\omega^2 \rho^{00}(\omega, k) = k^i k^j \rho^{ij}(\omega, k)$ implies that ρ_L vanishes at lightlike kinematics, $\mathcal{K}^2 = 0$.

- Introduce $(\lambda \in \mathbb{R})$

$$\rho(\omega, k, \lambda) = 2\rho_T + \lambda\, \rho_L \qquad \overset{\lambda=1}{=\!=} -\rho^\mu{}_\mu \ .$$

- Photon rate can be written $(\forall \lambda)$

$$d\Gamma_\gamma(\boldsymbol{k}) = \alpha\, \frac{d^3k}{4\pi^2\, k}\, \frac{\rho(k, k, \lambda)}{e^{\beta k} - 1}.$$

Choosing λ: weak and strong coupling spectral fcts

Spatial momentum $k = \pi T$: (see hep-th/0607237 and 1310.0164)

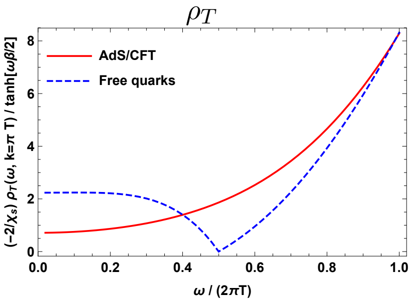

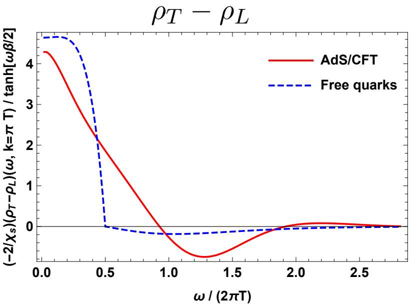

- ρ_T is positive-definite and free of the diffusion pole
- $(\rho_T - \rho_L)$ vanishes in the vacuum, is strongly suppressed at large ω and obeys a superconvergent sum-rule.
- At $\omega = k$, the two channels should be equal:
  non-trivial consistency check for lattice-based calculations!

Lattice QCD and vector correlators

Imaginary-time path-integral representation of QFT (Matsubara formalism).

Imaginary-time **vector correlators** ($\{\gamma^\mu,\gamma^\nu\} = 2g^{\mu\nu} = 2\mathrm{diag}(1,-1,-1,-1)$),

$$G^{\mu\nu}(x_0,\boldsymbol{k}) = \int d^3x\; e^{-i\boldsymbol{k}\cdot\boldsymbol{x}}\,\mathrm{Tr}\Big\{\frac{e^{-\beta H}}{Z(\beta)} j^\mu(x)\, j^\nu(0)\Big\}, \qquad j^\mu = \sum_f Q_f\,\bar\psi_f\gamma^\mu\psi_f$$

Spectral representation (u is a real four-vector): $\rightsquigarrow$ **inverse problem**

$$u_\mu G^{\mu\nu} u_\nu(x_0,\boldsymbol{k}) = \int_0^\infty \frac{d\omega}{2\pi}\; \underbrace{\frac{(u_\mu\rho^{\mu\nu}u_\nu)(\omega,\boldsymbol{k})}{\sinh(\beta\omega/2)}}_{\geq 0}\; \cosh[\omega(\beta/2 - x_0)].$$

Parameters of the lattice calculations

- $N_f = 2$ flavours of dynamical O(a) improved Wilson fermions with Wilson gauge action; ensembles generated with the openQCDv1.6 code.
- $T \simeq 254\,\mathrm{MeV}$, $L = 4/T \simeq 3.1\,\mathrm{fm}$; $m_\pi(T=0) \simeq 270\,\mathrm{MeV}$.
- Isovector current correlator is computed.

label	$(6/g_0^2, \kappa)$	$1/(aT)$	N_{conf}	$\frac{\mathrm{MDUs}}{\mathrm{conf}}$	$\tau_{\mathrm{int}}[Q^2(\bar{t})]$
F7	$(5.3, 0.13638)$	12	482	20	11.3(15)
O7	$(5.5, 0.13671)$	16	305	20	19(5)
W7	$(5.685727, 0.136684)$	20	1566	8	81(23)
X7	$(5.827160, 0.136544)$	24	511	10	490(230)

See 2001.03368 $(\rho_T - \rho_L)$, and 2205.02821 (ρ_T).

Continuum extrapolation of the $\rho_T - \rho_L$ Euclidean correlator

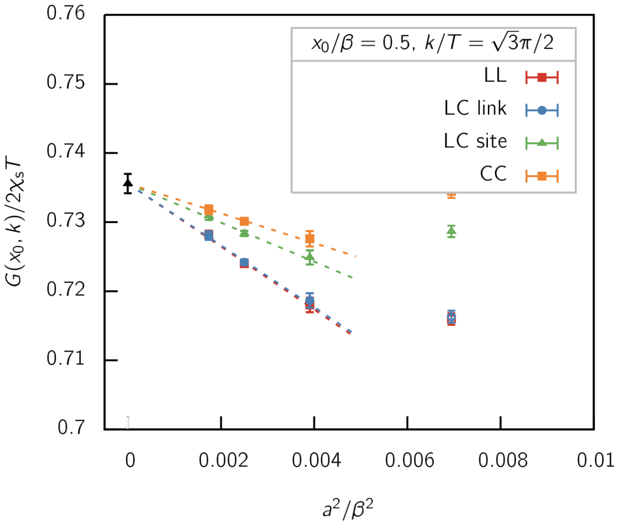

Analysis of the $(\rho_T - \rho_L)$ channel

'Hydrodynamics' prediction at small ω, k: with D the diffusion coefficient,

$$\rho(\omega, k, -2)/\omega \approx \frac{4\chi_s\, Dk^2}{\omega^2 + (Dk^2)^2} \qquad \omega, k \ll D^{-1}.$$

From the operator-product expansion:

$$\rho(\omega, k, \lambda = -2) \overset{\omega\to\infty}{\sim} k^2/\omega^4 \;\; : \qquad \int_0^\infty d\omega\, \omega\, \rho(\omega, k, -2) = 0.$$

$\rightsquigarrow$ 5-parameter ansatz:

$$\rho(\omega, k, -2) = \frac{A(1 + B\omega^2)\; \tanh(\omega\beta/2)}{[(\omega - \omega_0)^2 + b^2][(\omega + \omega_0)^2 + b^2][\omega^2 + a^2]}.$$

Analysis strategy: always determine B so as to satisfy the sum rule; scan over all other parameters to determine the χ^2 landscape.

For an early Backus-Gilbert analysis, see
Harris, Steinberg, Brandt, Francis, HM 1710.07050.

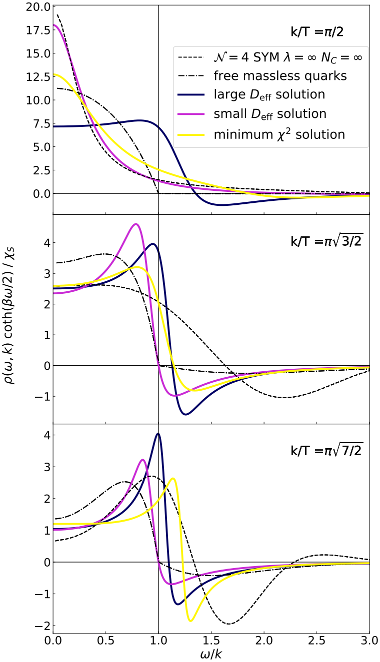

$\longleftarrow$ spec.funct. poorly constrained at small $k \simeq 0.4\,$GeV

Representative spectral functions describing the lattice $2(T-L)$ correlator

$\longleftarrow$ spec.funct. better constrained at $k \approx 2\pi T \simeq 1.6\,$GeV

Final result of analysis of the $(\rho_T - \rho_L)$ channel

$$D_{\text{eff}}(k) \equiv \frac{\rho(\omega = k, k, \lambda)}{4\chi_s k}, \qquad \chi_s = \beta \int d^3x \langle V_0(x) V_0(0) \rangle.$$

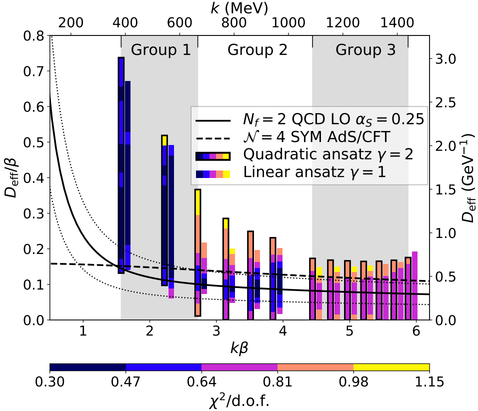

Cè et al. 2205.02821 (PRD).

Comparison of NLO+LPM spectral function to $T - L$ lattice data

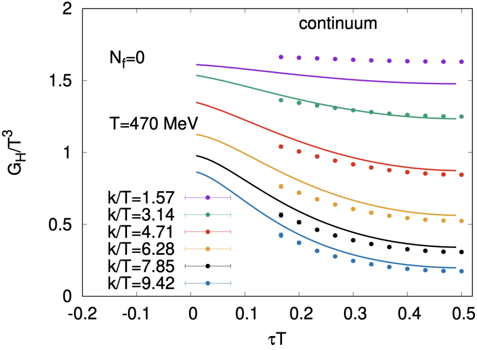

- Continuum-extrapolated quenched data from $N_t = 20, 24, 30$.
- General behaviour reproduced, but differences are visible.

2403.11647 Ali, Bala, Francis, Jackson, Kaczmarek, Turnwald, Ueding, Wink

The transverse channel

Cè et al. 2205.02821 (PRD).

Taking the continuum limit of $G_T(\tau, k)$

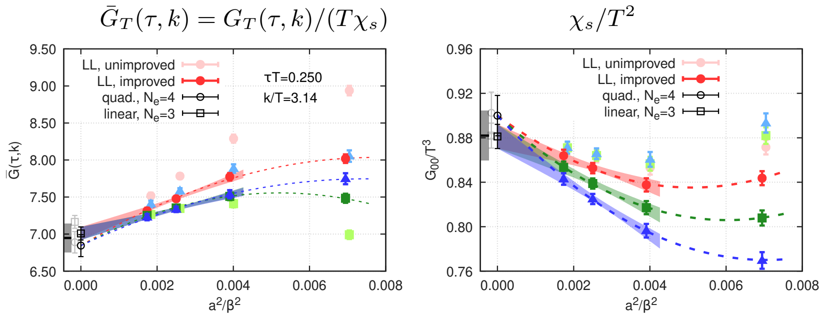

Three different discretisations, joint continuum extrapolation.

Use treelevel improvement.

Euclidean correlator: lattice vs. NLO prediction

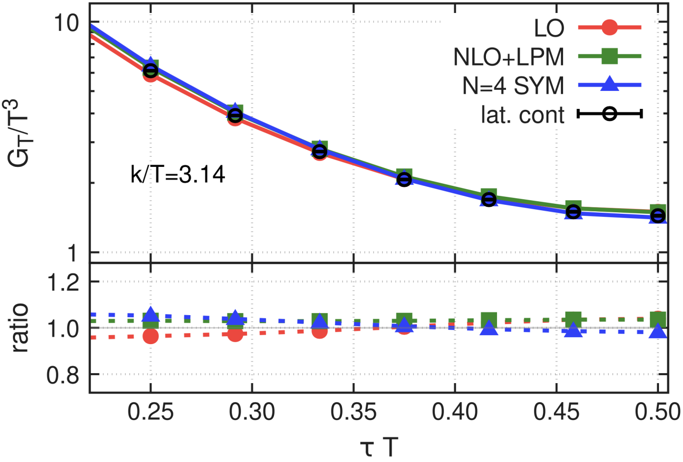

- NLO prediction lies a few percent higher than the lattice data.
- (For this comparison we set $\chi_s^{\rm AdS/CFT} = \frac{N_c^2 T^2}{8} \doteq \frac{9T^2}{8}$.)

(I) Backus-Gilbert spectral function

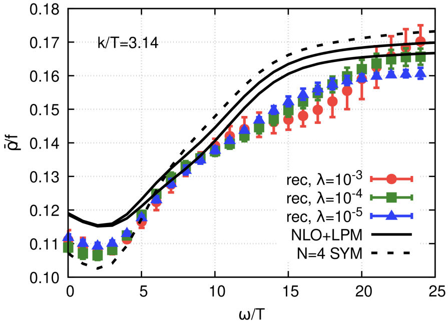

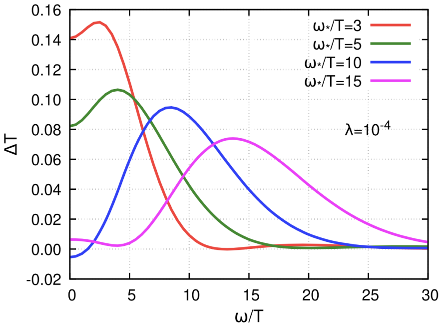

$$\frac{\bar{\rho}(\omega,k)}{f(\omega)} = \int_0^\infty d\omega'\ \Delta(\omega,\omega')\,\frac{\rho(\omega')}{f(\omega')} = \sum_i g_i(\omega) G_{\rm T}(\tau_i).$$

Choice made here: $f(\omega) = \frac{\omega^2}{\tanh(\beta\omega/2)}$ in order to make $\frac{\rho(\omega')}{f(\omega')}$ a 'slowly varying function', since the BG method is exact if $\frac{\rho(\omega')}{f(\omega')}$ is constant.

(II) Fit ansätze for the spectral functions

$$\rho(\omega) = \rho_{\rm fit}(\omega)(1 - \Theta(\omega, \omega_0, \Delta)) + \rho_{\rm pert}(\omega)\Theta(\omega, \omega_0, \Delta)$$

with $\omega_0 \approx 2.5\,$GeV the matching frequency,

$$\Theta(\omega, \omega_0, \Delta) = (1 + \tanh[(\omega - \omega_0)/\Delta])/2$$

a smooth step function and $\rho_{\rm pert}(\omega)$ from [Jackson, Laine 1910.09567].

A) Polynomial ansatz:

$$\frac{\rho_{\rm fit,1}(\omega)}{T^2} = \sum_{n=0}^{N_{\rm p}-1} A_n \left(\frac{\omega}{\omega_0}\right)^{1+2n},$$

B) Piecewise polynomial ansatz:

$$\frac{\rho_{\rm fit,2}(\omega)}{T^2} = \begin{cases} A_0\,\frac{\omega}{\omega_0} + A_1\left(\frac{\omega}{\omega_0}\right)^3, & \text{if } \omega \le k, \\ B_0\,\frac{\omega}{\omega_0} + B_1\left(\frac{\omega}{\omega_0}\right)^3, & \text{if } \omega > k. \end{cases}$$

Representative lattice-QCD results for the spectral functions

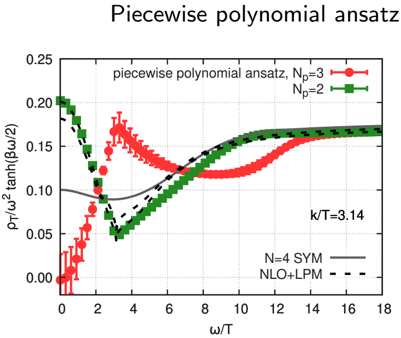

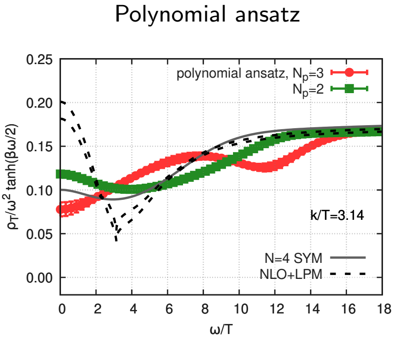

- Piecewise polynomial cannot ‘decide’ between having a min. or max. at $\omega = k$.
- Qualitatively, both the ‘AdS/CFT’ type and the ‘NLO’ type are compatible with the lattice data.

Final result for the photon emissivity

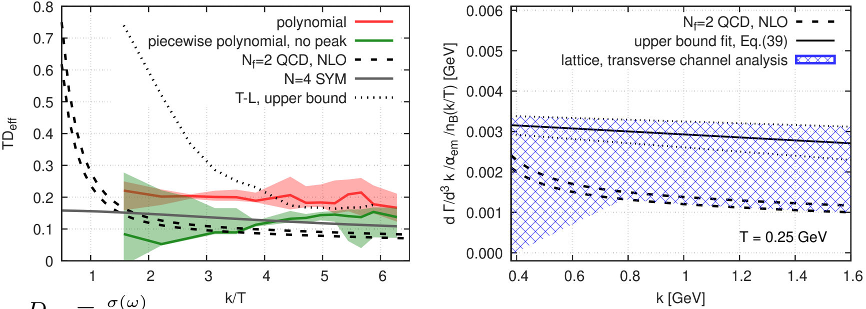

$D_{\rm eff} \equiv \frac{\sigma(\omega)}{2\chi_s k}$

- most fits give a larger photon emissivity than the weak-coupling prediction, but overall the lattice result is still compatible with it.
- the AdS/CFT prediction is also consistent with the lattice data for $k \gtrsim \pi T/2$.

2205.02821 Török et al.

Probing the photon emissivity without an inverse problem

Cè et al. 2309.09884 (PRD, Editor's Suggestion).

A dispersion relation for a Euclidean correlator at zero virtuality

- Let $\sigma(\omega) \equiv \rho_T(\omega, |\boldsymbol{k}| = \omega)$ be the spectral function proportional to the photon emissivity;

- let $H_E(\omega_n) \equiv G_E(\omega_n, k = i\omega_n)$ the momentum-space Euclidean correlator with Matsubara frequency $\omega_n = 2\pi T n$ and *imaginary* spatial momentum $k = i\omega_n$;

- once-subtracted dispersion relation: $(\sigma(\omega) \sim \omega^{1/2}$ at weak coupling)

$$H_E(\omega_n) = -\frac{\omega_n^2}{\pi} \int_0^\infty \frac{d\omega}{\omega} \, \frac{\sigma(\omega)}{\omega^2 + \omega_n^2} \,.$$

- these energy-moments of $\sigma(\omega)$ are directly accessible without involving an inverse problem.

HM, 1807.00781 (EPJC).

How different energy-moments probe $\sigma(\omega)$

$$H_E(\omega_n) - H_E(\omega_r) = \int_0^\infty \frac{d\omega}{\pi}\,\omega\left[\frac{1}{\omega^2+\omega_n^2} - \frac{1}{\omega^2+\omega_r^2}\right]\sigma(\omega).$$

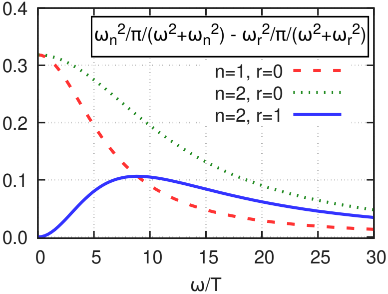

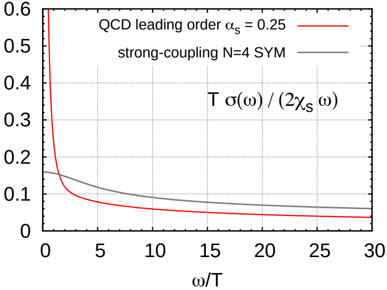

- $H_E(\omega_1)$ receives a sizeable contribution from the soft photons;
- $H_E(\omega_2) - H_E(\omega_1)$ probes the emission of hard photons.

Formulation on the lattice

Our standard representation: [Cè, . . . HM, 2112.00450]

$$H_E(\omega_n) = -\int_0^\beta dx_0 \int d^3x \, (e^{i\omega_n x_0} - e^{i\omega_n x_2}) \, e^{\omega_n x_3} \, \langle j_1(x) j_1(0) \rangle.$$

The $e^{i\omega_n x_2}$ term subtracts a static contribution which vanishes in the continuum (for the same reason the polarisation tensor component $\Pi_{11}(q)$ vanishes at lightlike virtuality for $q_1 = 0$).

- This representation has the advantage that $H_E(\omega_n)$ vanishes exactly in the vacuum even at finite lattice spacing;
- as a consequence, cutoff effects at finite temperature are strongly reduced.

NB. similar task to computing hadronic vacuum polarisation in muon $(g-2)$!

Computing $H_E(\omega_1)$

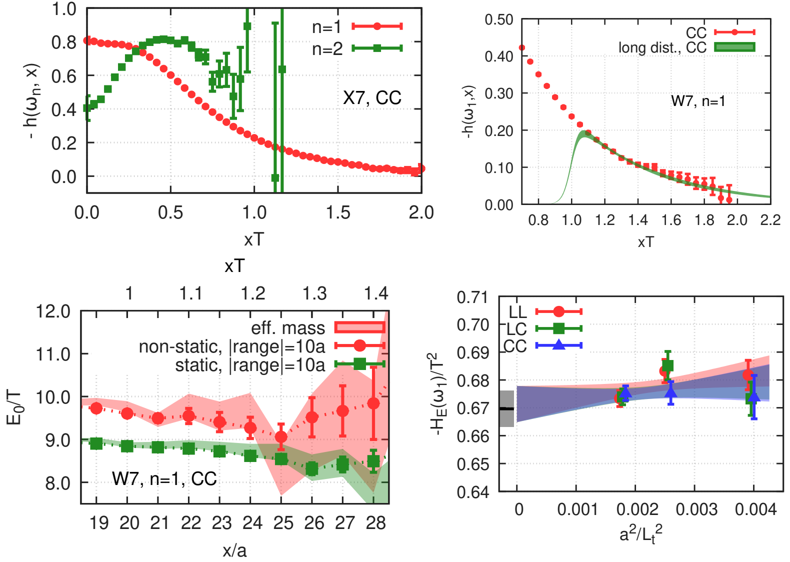

- $N_f = 2$, $T = 254\,$MeV, $N_t = 16, 20, 24$: Monte-Carlo chains were extended.

Result for $H_E(\omega_1)$: comparison to strong/weak-coupling predictions

Integrand to obtain $H_E(\omega_1)$

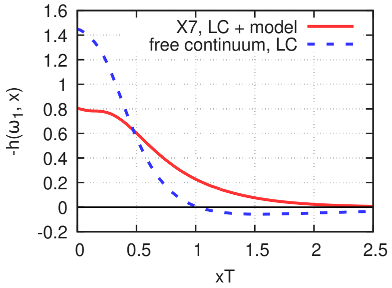

Comparison to theory predictions

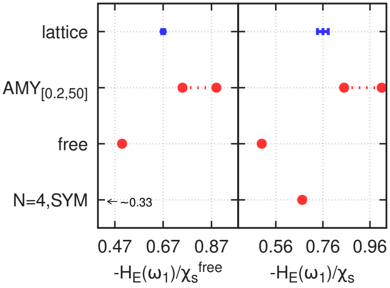

- $-H_E(\omega_1)$ turns out to be smaller than the value predicted from the AMY spectral function $\sigma(\omega)$; is it due to its peak around $\omega = 0$?
- for $H_E(\omega_2)$: better control of the large x_3 regime needed.

Cè et al, 2309.09884 (PRD).

Conclusion

- Photon rate: first lattice calculation in dynamical QCD with continuum limit.

- The transverse and the transverse-minus-longitudinal channels show small but statistically significant deviations from the state-of-the-art weak-coupling calculations at $T = 254\,\text{MeV}$;

- Treatment of the inverse problem with Backus-Gilbert method or with an explicit fit ansatz for $\sigma(\omega)$ leads to consistent results for the photon emissivity for $\pi T \lesssim \omega \lesssim 2\pi T$.

- Those results are still compatible with weak-coupling prediction and AdS/CFT.

- Dispersion relation at fixed photon virtuality $q^2 = 0$: $H_E(\omega_1)$ is lower than the value derived from the weak-coupling spectral function $\sigma(\omega)$; the perturbative uncertainty is now the limiting factor.

Thermal modification of vector spectral function [Krasniqi et al. 2407.01657]

- Quasi physical-mass $N_f = 2+1$ simulations, $m_\pi(T=0) = 130\,\text{MeV}$; parameters of CLS ensemble E250, $L = 6.1\,\text{fm}$, $a \simeq 0.064\,\text{fm}$.
- 3 ensembles: $N_t = 24, 20, 16$ corresponding to temperatures 128, 154 and 192 MeV.
- among other observables, we studied (at $\boldsymbol{p} = 0$; isovector vector and axial-vector channels)

$$G(x_0, \boldsymbol{p}, T) - \sum_{n\in\mathbb{Z}} G(|x_0 + n\beta|, \boldsymbol{p}, 0)$$

$$= \int_0^\infty d\omega \, \Big(\underbrace{\rho(\omega, \boldsymbol{p}, T) - \rho(\omega, \boldsymbol{p}, 0)}_{\equiv \Delta\rho(\omega,\boldsymbol{p},T)} \Big) \frac{\cosh[\omega(\frac{\beta}{2} - x_0)]}{\sinh[\frac{\beta}{2}\omega]}.$$

Used Backus-Gilbert method with rescaling function $f(\omega) = \omega$ to constrain $\Delta\rho(\omega, \boldsymbol{p}, T)$.

NB. $\Delta\rho(\omega, \boldsymbol{p}, T) \overset{\omega\to\infty}{\sim} 1/\omega^2$.

Reminder: vacuum spectral functions from τ decays

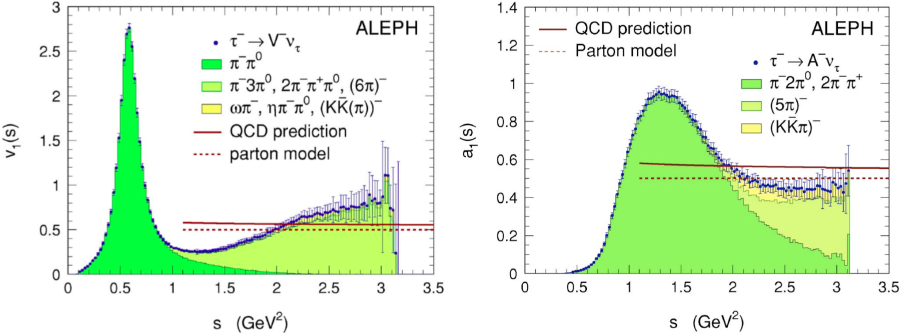

NB. $\rho_V(\omega, \mathbf{0}, T) = \frac{\omega^2}{4\pi^2} v_1(\omega^2)$

Fig. from Davier, Höcker, Zhang, doi:10.1103/RevModPhys.78.1043

Results of BG analysis

Vector | Axial-vector

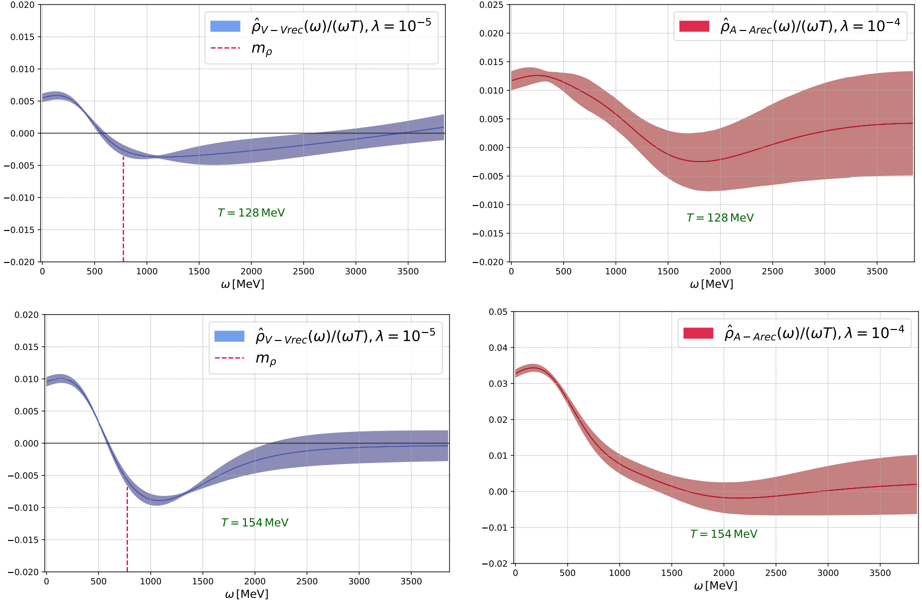

Spectral sum rules

$$\int_0^\infty \frac{d\omega}{\omega}\,\Delta\rho_V(\omega,\mathbf{0},T) = 0. \qquad [1107.4388]$$

- generically, a transport peak appears in the spectral function at $\omega = 0$, and therefore the contribution of the ρ meson must be reduced in order to satisfy the sum rule [Brandt, Francis, Jäger, HM 1512.07249]

$$\begin{aligned}\int_0^\infty \frac{d\omega}{\omega}\,\Delta\rho_A(\omega,\mathbf{0},T) &= G_A(\omega_n=0,\boldsymbol{p}=0,T) - G_A(0,\mathbf{0},0)\\ &= f_\pi^2(T=0) - f_\pi^2(T) + \mathrm{O}(m_q^2)\end{aligned}$$

- $f_\pi(T)$, the decay constant of the 'static screening pion', falls off monotonously with increasing temperature;
  it is $\mathrm{O}(m_q)$ in the chirally restored phase.
- Thus the RHS

Ensembles used for computing $H_E(\omega_1)$ and $H_E(\omega_2)$

label	$6/g_0^2$	κ	L_t/a	N_{conf}	$\frac{\mathrm{MDUs}}{\mathrm{conf}}$
O7	5.5	0.13671	16	1500	20
W7	5.685727	0.136684	20	1600	8
X7	5.827160	0.136544	24	2012	10

2309.09884

Motivation: some heavy-ion collision phenomenology

- direct photons (those not produced via hadronic decays) encode information about the environment in which they were created
- for $1\text{GeV} \lesssim p_T \lesssim 2\text{GeV}$: expect a sizeable contribution from thermal photons: quark-gluon plasma and hadronic phase
- RHIC, $\sqrt{s_{NN}} = 200\,$GeV:
  - PHENIX measurement of $p_T < 3\,$GeV photons shows clear excess over $N_{\rm coll}$-scaled pp measurement [PRL 104, 132301 (2010)]
  - PHENIX: large photon anisotropy wrt reaction plane [PRL 109, 122302 (2012)]
  - STAR: photon yield ~ 3 times smaller than PHENIX: unresolved tension
  - PHENIX: higher-statistics study [PRC 109, 044912 (2024)]
- LHC, $\sqrt{s_{NN}} = 2760\,$GeV: ALICE measured photon yield [PLB 754, 235 (2016)].
- recently, ALICE measured dileptons at $\sqrt{s_{NN}} = 5020\,$GeV, in particular determining direct photon yield [2308.16704]

Phenomenology: Gale et al. [2106.11216]. Review G. David [1907.08893].

Lattice papers on the photon rate

- Karsch, Laermann, Petreczky, Stickan, Wetzorke 2002; S. Gupta 2004; Aarts, Allton, Foley, Hands, Kim 2007: quenched calculations, $k = 0$.
- hep-lat/0610061 (LAT06): Aarts, Allton, Foley, Hands: quenched, $k \neq 0$
- 1012.4963 (PRD): Ding, Francis, Kaczmarek, Karsch, Laermann, Soeldner, quenched calculation with continuum limit, $k = 0$.
- 1212.4200 (JHEP): Brandt, Francis, HM, Wittig: $N_f = 2$, $N_t = 16$, $k = 0$, $m_\pi = 270$, $T = 250$MeV.
- 1307.6763 (PRL), 1412.6411 (JHEP): Aarts, Allton, Amato,Giudice, Hands, Skullerud: $N_f = 2 + 1$, $k = 0$, anisotropic, fixed-scale temperature scan, $m_\pi = 384\,$MeV
- 1512.07249 (PRD): Brandt, Francis, Jäger, HM, $N_f = 2$, $k = 0$, $N_t = 12 \to 24$, $m_\pi = 270$, fixed-scale scan across the phase transition.
- 1604.07544 (PRD): Ghiglieri, Kaczmarek, Laine, F. Meyer: quenched calculation with continuum limit, $k \neq 0$.
- 2001.03368 (PRD): Cè, Harris, HM, Steinberg, Toniato, $N_f = 2$ calculation with continuum limit at $T = 250$MeV, $k \neq 0$; transv-minus-longitud. channel.
- 2205.02821 (PRD): idem, but transverse channel.
- 2309.09884 (PRD): Cè, Harris, Krasniqi, HM, Török, calculation of energy-moments at zero virtuality.
- 2403.11647: Ali, . . . Francis, Kaczmarek et al.: analysis of transv-minus-longitud. channel.

Results for the effective diffusion coefficient $D_{\text{eff}} \equiv \frac{\rho_T(\omega=k,k)}{2\chi_s k}$

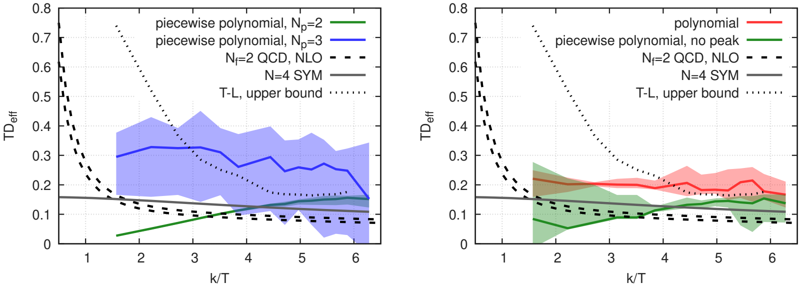

- left panel: comparison with results of $(T-L)$ channel analysis: piecewise-polynomial ansatz with max. at $\omega = k$ is disfavoured for $k \geq \pi T$.
- right panel: forbidding a max. at the 1σ level, predictivity is much stronger.
- polynomial ansatz favours values even larger than the $\mathcal{N}=4$ SYM prediction from AdS/CFT (hep-th/0607237).

Representation through non-static screening masses

$$\tilde{G}_E(\omega_r, x_3) = -2\int_0^\beta dx_0\; e^{i\omega_r x_0} \int dx_1 dx_2\; \langle J_1(x) J_1(0)\rangle = \sum_n |A_n^{(r)}|^2 e^{-E_n^{(r)}|x_3|}$$

$$\Rightarrow \underbrace{H_E(\omega_r)}_{=\mathrm{O}(g^2)} \equiv \int_{-\infty}^{\infty} dx_3\; \tilde{G}_E(\omega_r, x_3)\; e^{\omega_r x_3} = 2\omega_r^2 \sum_{n=0}^{\infty} \underbrace{|A_n|^2}_{=\mathrm{O}(g^4)}\; \underbrace{\frac{1}{E_n^{(r)}\,(E_n^{(r)2} - \omega_r^2)}}_{=\mathrm{O}(g^{-2})}.$$

This helps explain the connection observed in [Brandt et al, 1404.2404] between non-static screening masses and the LPM-resummation contributions to the photon emission rate [Aurenche et al, hep-ph/0211036].

Sketch of the (standard) derivation of the dispersion relation

$G_R(\omega,k) = i(\delta_{il} - \frac{k_i k_l}{k^2}) \int d^4x\, e^{i\mathcal{K}\cdot x}\theta(x^0) \left\langle [\mathrm{j}^i(x),\, \mathrm{j}^l(0)] \right\rangle$. But

$$[j^\mu(x), j^\nu(0)] = 0 \quad \text{for} \quad x^2 < 0,$$

$\Rightarrow$ the retarded correlator $H_R(\omega) \equiv G_R(\omega, k=\omega)$ at lightlike momentum is analytic for $\mathrm{Im}\,(\omega) > 0$. Similarly, the advanced correlator $H_A(\omega)$ is analytic for $\mathrm{Im}\,(\omega) < 0$.

Define the function $H(\omega) = \begin{cases} H_R(\omega) & \mathrm{Im}\,(\omega) > 0 \\ H_A(\omega) & \mathrm{Im}\,(\omega) < 0 \end{cases}$.
It is analytic everywhere, except for a discontinuity on the real axis:

$$H(\omega + i\epsilon) - H(\omega - i\epsilon) = H_R(\omega) - H_A(\omega) = i\sigma(\omega),$$

Write a Cauchy contour-integral representation (using two half-circles) of $H(\omega)$ just above the real axis, where it coincides with $H_R(\omega)$:

$$H_R(\omega) = H_R(\omega_r) + \int_{-\infty}^{\infty} \frac{d\omega'}{2\pi}\, \sigma(\omega') \Big[\frac{1}{\omega' - \omega - i\epsilon} - \frac{1}{\omega' - \omega_r - i\epsilon}\Big].$$

The dispersion relation for the Euclidean correlator follows from the observation $G_E(\omega_n, k^2) = G_R(i\omega_n, k^2), \qquad n > 0.$